

Real Time Waveguide Parameter Estimation Using Sparse Multimode Disperse Radon Transform

Claudio Araya¹, Alejandro Martinez¹, Donatien Ramiandrisoa², Dean Ta³,
Kailiang Xu³, Axel Osses⁴, and Jean-Gabriel Minonzio^{1,5}

¹*Escuela de Ingeniería Informática, Universidad de Valparaíso, Chile.*

²*Bleu Solid, Pomponne, France.*

³*Center for Biomedical Engineering, School of Information Science and Technology,
Fudan University, Shanghai, China.*

⁴*Departamento de Ingeniería Matemática, CMM UMI CNRS 2807, Universidad de Chile, Santiago, Chile.*

⁵*Centro de Investigación y Desarrollo en Ingeniería en Salud, Universidad de Valparaíso, Chile.*

Abstract—Osteoporosis and associated fragility fractures are still a societal problem. Several quantitative ultrasound approaches have been proposed to overcome limitations of the current gold standard DXA. Bi Directional Axial Transmission (BDAT) is based on the measurement of waves guided by the cortical bone shell. Cortical thickness (Ct.Th) and porosity (Ct.Po) estimates correspond to the maxima of the objective function $\text{Proj}(\text{Ct.Th}, \text{Ct.Po})$, initially defined as the projection of a tested model in the singular vector basis (method 1). Each model matrix has the same dimension, i.e., $N_f=124 \times N_k=256$, 512, 1024 or 2048 pixels, of an ultrasonic guided wave spectrum experimental image $\text{Norm}(f, k)$. The total number of models is equal to $N_{th}=38 \times N_{po}=25$, i.e., the number of cortical thickness and porosity taken into account, ranging respectively from 0.8 to 4.5 mm and 1 to 25%. Finally, each pixel of the alternative objective function ($N_{th} \times N_{po}$ pixels) corresponds to the pixel-wise image multiplication between one model and the experimental guided wave spectrum image (method 2) or a sparse matrix multiplication between experimental and model reshaped vectors (method 3). The three methods were tested on data obtained on 400 measurements. It was observed that methods 2 and 3 provided the same Ct.Th Ct.Po values while differences with method 1 decreased with N_k . Acceptable differences, i.e., lower than the typical measurement resolution (0.2 mm for Ct.Th and 1% for Ct.Po) were achieved for $N_k=2048$. Using Matlab on a standard desktop, this calculation took 20, 4 and 0.3 s, for the methods 1 to 3, respectively. Method 3 calculation was achieved in 5 ms using C++. This last value opens perspective toward guiding interface improvement using real time objective function.

Index Terms—Ultrasonic guided waves, cortical bone, real time guiding interface, pixel-wise image multiplication, sparse matrix multiplication

I. INTRODUCTION

Osteoporosis is recognized as a skeletal disorder, caused by an imbalance in bone remodeling, which is influenced by the genetic code and several other factors, including the adequate level of physical, hormonal, and nutritional activity [1], [2]. Osteoporotic bone has increased porosity and decreased thickness that increases the risk of fracture. Worldwide, 1.6 million hip fractures occur annually and are expected to increase to 6.3 million by 2050 [3]. In addition, 1 in 3 women and 1 in 5

men over 50 years are expected to suffer from an osteoporotic fracture [2].

Currently, the *gold standard* for fracture risk assessment is dual-energy X-ray absorptiometry (DXA) [4], [5]. This technique generates a calibrated gray level image by applying a small dose of X-rays. This image provides bone mineral density by area as well as its normalized T-score counterpart. In fact, osteoporosis in adults is diagnosed on the basis of a T-score equal to or lower than -2.5. However, most people who suffer fragility fractures are above this limit [6], [7]. On the other hand, DXA has the disadvantage of its large volume and cost, making it difficult to access a large part of the world's population such as in Latin America [8].

Within ultrasound techniques [9], alternatives such as vibroacoustic [10], imaging [11], back scattering [12] have been recently proposed. The ultrasonic alternative used in this study is the bidirectional axial transmission device (BDAT) [13], measuring the propagation of guided waves at 1 MHz, with a wavelength comparable to the cortical thickness [14]. In particular, the SVD-based method applied to multiple transmitters and receiver provides a guided wave spectrum image (GWSI), initially denoted $\text{Norm}(f, k)$ [15]. This approach has been generalized to an inverse problem scheme, denoted objective function, which maxima position correspond to cortical porosity (Ct.Po) and cortical thickness (Ct.Th) estimates. However, this approach tends to fail for patients associated with either poor guided mode information [16] or difficulties for *in vivo* probe alignment [16]. Thus, the development of robust and fast inverse problem is a key parameter to success of the device.

Several methods have been proposed for the assessment of anisotropic plate properties [17], [18] using the dispersive [19] and sparse [20] properties of guided waves. The objective function used in this study is based on a 2D-transverse isotropic free plate model [21], with the elasticity parametrized with porosity considering a fixed bone matrix [22]. The objective of the study is to proposed two alternatives methods to the objective functions and to compare their results and calculation times.

II. MATERIALS AND METHODS

A. Method 1

The first method has proposed in Ref. [16] and will be used as a reference in the following. It has been initially introduced as a generalisation of the so-called *Norm* function obtained through a SVD-enhanced 2-D spatio-temporal Fourier transform [15] and also called guided wave spectrum image [23]. Each pixel corresponds to the projection of testing vector into the reception singular basis [15]. The testing vector spans all the waves measurable by the device, corresponding to all frequencies f and wave numbers k within the device bandwidth. Thus, each pixel (f, k) of the *Norm* function reflects in a 0-1 scale the presence rate of the tested plane wave in the measured signals.

In the case of the objective function, instead of spanning all measurable waves, the testing vectors are limited to the guided modes of the model [16], [24]. This approach takes advantage of the sparsity of the (f, k) domain, i.e., for a considered model, only a finite number M of guided mode wave numbers $k_m(f, Ct.Th, Ct.Po)$ are present at each frequency [25]. Each pixel of the objective function reflects in a 0-1 scale the presence rate of the tested model in the measured signals. Thus, the optimal model parameters $Ct.Th$ and $Ct.Po$ can be found by maximizing the objective function. An example of objective function is shown in Fig. 1. This point of view can be interpreted as a multimode Disperse Radon Transform [26]. However, this formulation prevented fast calculation for real application. The reference time for method 1 is 20 s. In the following, two alternative formulations of the objective function are proposed.

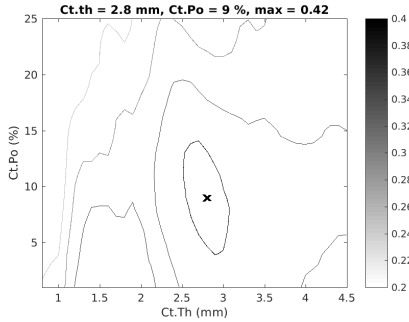


Fig. 1. Method 1: A pixel of the objective function ($Nth \times Npo$ pixels) corresponds to the projection of a tested model in the singular vector basis [16].

B. Method 2

The waveguide models are stored as sparse matrices, i.e., containing few non zero values corresponding to the theoretical guided mode positions in the frequency f , wavenumber k plane. The value of the pixel is equal to 1 divided by the number of theoretical modes at one frequency. Each model matrix has the same dimension, i.e., $Nf=124 \times Nk=256, 512, 1024$ or 2048 pixels, of an ultrasonic guided wave spectrum experimental image $Norm(f, k)$. The total number of models

is equal to $Nth=38 \times Npo=25$, i.e., the number of cortical thickness and porosity taken into account, ranging respectively from 0.8 to 4.5 mm and 1 to 25%. Finally, each pixel of the alternative objective function ($Nth \times Npo$ pixels) corresponds to the pixel-wise image multiplication between one model and the experimental guided wave spectrum image (method 2). Both images have indeed the same dimension: $Nf \times Nk$. An example of multiplication of a guided wave spectrum image and a wave guided image is shown in Fig. 2.

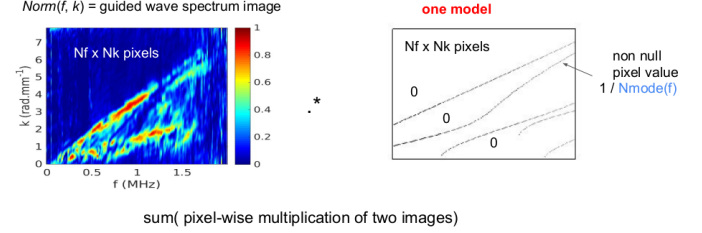


Fig. 2. Method 2: A pixel of the alternative objective function ($Nth \times Npo$ pixels) corresponds to the pixel-wise image multiplication between one model and the experimental guided wave spectrum image.

The main difference with method 1 is that the m^{th} guided mode wavenumber $k_m^{th}(f)$ at frequency f is approximated to the closed wavenumber value of the sampled k vector. In method 1, exact guided mode wavenumber are taken into account. That is why, difference resolution for the k vector are considered: $Nk=256, 512, 1024$ and 2048 . The number of frequencies Nf remains equal to 124, for considered frequencies ranging to 0.4 to 1.6 MHz.

C. Method 3

In the second method, a loop on the models is necessary to achieve the complete alternative objective function. The idea behind the third method is obtain the same results using less computation. To this end, image dimensions and reshaped matrices are taken into account following Orthogonal Matching Pursuit approach [27]. Principle is described in Fig. 3. First, both guided wave spectrum image and model database are reshaped. The guided wave spectrum image is reshaped from a 2D $Nf \times Nk$ matrix to a 1D $1 \times (Nf \cdot Nk)$ vector. Likewise, the model database is reshaped from a 4D to a 2D matrix, which dimensions are $(Nf \cdot Nk) \times (Nth \cdot Npo)$. Thus, the matrix product between two previous vector and matrix is a $1 \times (Nth \cdot Npo)$ vector, which can be reshaped into a $Nth \times Npo$ objective function. Two multiplications will be considered: classical and sparse matrix multiplication [28]. The three methods were tested on data obtained on 400 *in vivo* measurements.

III. RESULTS

It was observed that methods 2 and 3 provided the same $Ct.Th$ $Ct.Po$ values while differences with method 1 decreased with Nk . Acceptable differences, i.e., lower than the typical measurement resolution (0.2 mm for $Ct.Th$ and 1% for $Ct.Po$ [24]) were achieved for $Nk=2048$.

ACKNOWLEDGMENT

Jean-Gabriel Minonzio (JGM) and Axel Osses (AO) are supported by Grant ANID / FONDECYT / REGULAR / 1201311. AO was partially funded by ANID-Fondecyt Grants 1191903 and 1201311, Basal Program CMM-AFB 170001, FONDAP/15110009, Millennium Science Initiative Programs NCN17_1 and NCN19_161, Math-Amsud Project ACIPDE MATH190008 and ECOS 200061.

REFERENCES

- [1] M. Sinaki, "Osteoporosis," in *Braddom's Physical Medicine and Rehabilitation*. Elsevier, 2021, pp. 690–714.e3. [Online]. Available: <https://doi.org/10.1016/b978-0-323-62539-5.00034-5>
- [2] E. M. Curtis, R. J. Moon, N. C. Harvey, and C. Cooper, "The impact of fragility fracture and approaches to osteoporosis risk assessment worldwide," *Bone*, vol. 104, pp. 29–38, Nov. 2017. [Online]. Available: <https://doi.org/10.1016/j.bone.2017.01.024>
- [3] P. Sambrook and C. Cooper, "Osteoporosis," *The Lancet*, vol. 367, no. 9527, pp. 2010–2018, Jun. 2006. [Online]. Available: [https://doi.org/10.1016/s0140-6736\(06\)68891-0](https://doi.org/10.1016/s0140-6736(06)68891-0)
- [4] G. M. Blake and I. Fogelman, "The role of DXA bone density scans in the diagnosis and treatment of osteoporosis," *Postgraduate Medical Journal*, vol. 83, no. 982, pp. 509–517, Aug. 2007.
- [5] I. Khatik, "A study of various bone fracture detection techniques," *International Journal Of Engineering And Computer Science*, Jun. 2017.
- [6] P. Choksi, K. J. Jepsen, and G. A. Clines, "The challenges of diagnosing osteoporosis and the limitations of currently available tools," *Clinical Diabetes and Endocrinology*, vol. 4, no. 1, May 2018. [Online]. Available: <https://doi.org/10.1186/s40842-018-0062-7>
- [7] E. Lespessailles, B. Cortet, E. Legrand, P. Guggenbuhl, and C. Roux, "Low-trauma fractures without osteoporosis," *Osteoporosis International*, vol. 28, p. 1771–1778, 2017.
- [8] S. S. Maeda, R. D. S. LLibre, H. P. Arantes, G. C. de Souza, F. F. C. Molina, D. Wiluzanski, J. A. C. Tabora, C. C. Montaña, T. M. Vargas, G. L. F. Lopez, L. V. Neira, G. A. M. Uribe, D. Salica, A. R. Bencosme, S. C. Perez, C. R. R. Acosta, J. J. Carey, and J. L. C. Borges, "Challenges and opportunities for quality densitometry in latin america," *Archives of Osteoporosis*, vol. 16, no. 1, p. 23, Feb. 2021. [Online]. Available: <https://doi.org/10.1007/s11657-021-00892-y>
- [9] S. Behforootan, O. Boughton, U. Hansen, J. Cobb, P. Huthwaite, and R. Abel, "Ultrasound and bone disease: A systematic review," *World Journal of Surgery and Surgical Research*, vol. 4, p. 1296, 2021.
- [10] P. Agnollitto, G. Braz, A. Spirlandeli, F. Albuquerque de Paula, A. A. Carneiro, and M. Nogueira-Barbosa, "Ex vivo vibro-acoustography characterization of osteoporosis in an experimental mice model," *Quantitative Imaging in Medicine and Surgery*, vol. 11, pp. 586–596, 2021.
- [11] G. Renaud, P. Clouzet, D. Cassereau, and M. Talmant, "Measuring anisotropy of elastic wave velocity with ultrasound imaging and an autofocus method - application to cortical bone," *Physics in medicine and biology*, vol. 65, p. 23, 2020.
- [12] G. Armbrrecht, H. Nguyen Minh, J. Massmann, and K. Raum, "Pore-size distribution and frequency-dependent attenuation in human cortical tibia bone discriminate fragility fractures in postmenopausal women with low bone mineral density," *JBMR Plus*, vol. n/a, no. n/a, p. e10536, 2021, e10536 JBMR4-07-21-0087. [Online]. Available: <https://asbmr.onlinelibrary.wiley.com/doi/abs/10.1002/jbmr4.10536>
- [13] E. Bossy, M. Talmant, M. Defontaine, F. Patat, and P. Laugier, "Bidirectional axial transmission can improve accuracy and precision of ultrasonic velocity measurement in cortical bone: a validation on test materials," *IEEE Transactions on Ultrasonics, Ferroelectrics and Frequency Control*, vol. 51, no. 1, pp. 71–79, jan 2004.
- [14] K. Xu, D. Ta, D. Cassereau, B. Hu, W. Wang, P. Laugier, and J.-G. Minonzio, "Multichannel processing for dispersion curves extraction of ultrasonic axial-transmission signals: Comparisons and case studies," *J Acoust Soc Am*, vol. 140, no. 3, pp. 1758–1770, 2016.
- [15] J.-G. Minonzio, M. Talmant, and P. Laugier, "Guided wave phase velocity measurement using multi-emitter and multi-receiver arrays in the axial transmission configuration," *The Journal of the Acoustical Society of America*, vol. 127, no. 5, pp. 2913–2919, may 2010.

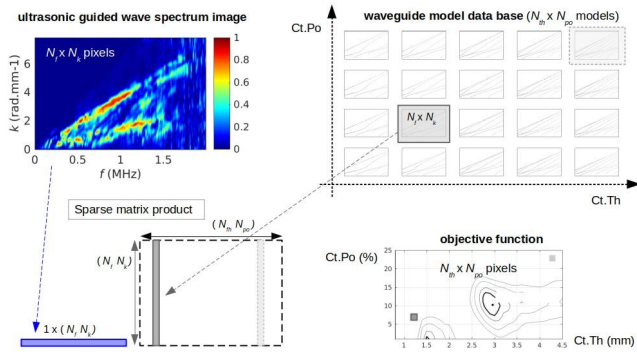


Fig. 3. Method 3: A pixel of the objective function ($N_{th} \times N_{po}$ pixels) corresponds to a sparse matrix multiplication between experimental and model reshaped vectors.

Calculation times are provided in Fig. 4. As expected, it can be observed that the times increase with Nk . Compared to the reference time of method 1 (20 s), methods 2 and 3 are quicker. Using Matlab on a standard desktop, method 2, based on image products, needs 4 s for $Nk = 2048$. Likewise, method 3, based on a single matrix product and reshaped, is 8 times faster in the same condition. The same calculation has been tested in C++ with a 5 time gain. Finally, the smallest calculation time, i.e. 5 ms, was achieved in C++ using the sparse matrix multiplication point of view. Compared to method 1, the total time gain is about 5000.

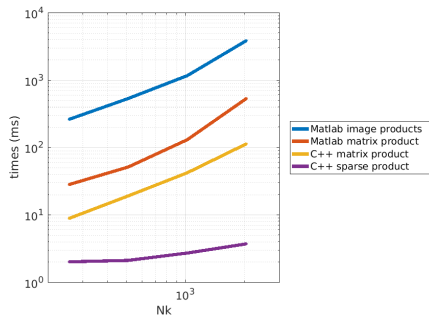


Fig. 4. Comparison of the calculation times of the three methods using Matlab and C++ in function of Nk

IV. CONCLUSIONS

The context of this study is the development of a clinical BDAT prototype, based on the measurement of ultrasonic guided waves in cortical bone. The aim is to achieve a robust and easy to use measurement. The novel formulations of the inverse problem objective function, allowing to obtain estimates of cortical thickness and porosity, lead to a typical calculation time of 5 ms. This result opens a perspective toward guiding interface improvement using real-time objective function. This approach will be soon integrated into the interface device.

- [16] J.-G. Minonzio, N. Bochud, Q. Vallet, Y. Bala, D. Ramiandrisoa, H. Follet, D. Mitton, and P. Laugier, "Bone cortical thickness and porosity assessment using ultrasound guided waves: An *ex vivo* validation study," *Bone*, vol. 116, pp. 111–119, Nov. 2018.
- [17] N. Bochud, J. Laurent, F. Bruno, D. Royer, and C. Prada, "Towards real-time assessment of anisotropic plate properties using elastic guided waves," *The Journal of the Acoustical Society of America*, vol. 143, no. 2, pp. 1138–1147, 2018. [Online]. Available: <https://asa.scitation.org/doi/abs/10.1121/1.5024353>
- [18] Q. Chen, K. Xu, and D. Ta, "High-resolution lamb waves dispersion curves estimation and elastic property inversion," *Ultrasonics*, vol. 115, p. 106427, 2021. [Online]. Available: <https://www.sciencedirect.com/science/article/pii/S0041624X21000664>
- [19] S. Chen, K. Wang, Z. Peng, C. Chang, and W. Zhai, "Generalized dispersive mode decomposition: Algorithm and applications," *Journal of Sound and Vibration*, vol. 492, p. 115800, 2021. [Online]. Available: <https://www.sciencedirect.com/science/article/pii/S0022460X20306295>
- [20] Y. Hu, F. Cui, F. Li, X. Tu, and L. Zeng, "Sparse wavenumber analysis of guided wave based on hybrid lasso regression in composite laminates," *Structural Health Monitoring*, vol. 0, no. 0, p. 14759217211032118, 0. [Online]. Available: <https://doi.org/10.1177/14759217211032118>
- [21] J. Foiret, J.-G. Minonzio, C. Chappard, M. Talmant, and P. Laugier, "Combined estimation of thickness and velocities using ultrasound guided waves: a pioneering study on *in vitro* cortical bone samples," *IEEE Trans Ultrason Ferroelectr Freq Control*, vol. 61, pp. 1478–1488, 2014.
- [22] N. Bochud, Q. Vallet, Y. Bala, H. Follet, J.-G. Minonzio, and P. Laugier, "Genetic algorithms-based inversion of multimode guided waves for cortical bone characterization," *Physics in Medicine and Biology*, vol. 61, pp. 6953–6974, 09 2016.
- [23] J.-G. Minonzio, B. Cataldo, R. Olivares, D. Ramiandrisoa, R. Soto, B. Crawford, V. H. C. De Albuquerque, and R. Munoz, "Automatic classifying of patients with non-traumatic fractures based on ultrasonic guided wave spectrum image using a dynamic support vector machine," *IEEE Access*, vol. 8, pp. 194752–194764, 2020.
- [24] J.-G. Minonzio, N. Bochud, Q. Vallet, D. Ramiandrisoa, A. Etchet, K. Briot, S. Kolta, C. Roux, and P. Laugier, "Ultrasound-based estimates of cortical bone thickness and porosity are associated with non-traumatic fractures in postmenopausal women: A pilot study," *Journal of Bone and Mineral Research*, vol. 34, no. 9, pp. 1585–1596, Mar. 2019.
- [25] K. Xu, J.-G. Minonzio, D. Ta, B. Hu, W. Wang, and P. Laugier, "Sparse svd method for high-resolution extraction of the dispersion curves of ultrasonic guided waves," *IEEE transactions on ultrasonics, ferroelectrics, and frequency control*, vol. 63, no. 10, pp. 1514–1524, 2016.
- [26] K. Xu, P. Laugier, and J.-G. Minonzio, "Dispersive radon transform," *J Acoust Soc Am*, vol. 143, pp. 2729–2743, 2018.
- [27] J. A. Tropp and A. C. Gilbert, "Signal recovery from random measurements via orthogonal matching pursuit," *IEEE Transactions on Information Theory*, vol. 53, no. 12, pp. 4655–4666, 2007.
- [28] R. Yuster and U. Zwick, "Fast sparse matrix multiplication," vol. 1, 2005, pp. 2–13.